EML 4905 Senior Design Project

A B.S. THESIS
PREPARED IN PARTIAL FULFILLMENT OF THE
REQUIREMENT FOR THE DEGREE OF
BACHELOR OF SCIENCE
IN
MECHANICAL ENGINEERING

FSAE 2015 Chassis and Suspension 25% Report

Alejandro Diaz
Osvaldo Fernandez
Ricardo Gonzalez
Christian Ramos

Advisor: Professor Andres Tremante

March 17, 2014

This B.S. thesis is written in partial fulfillment of the requirements in EML 4905. The contents represent the opinion of the authors and not the Department of Mechanical and Materials Engineering.

Ethics Statement and Signatures

The work submitted in this B.S. thesis is solely prepared by a team consisting of Alejandro Diaz, Osvaldo Fernandez, Ricardo Gonzalez, and Christian Ramos and it is original. Excerpts from others' work have been clearly identified, their work acknowledged within the text and listed in the list of references. All of the engineering drawings, computer programs, formulations, design work, prototype development and testing reported in this document are also original and prepared by the same team of students.

Alejandro Diaz	Osvaldo Fernandez	Ricardo Gonzalez	Christian Ramos
Team Leader	Team Member	Team Member	Team Member

Dr. Andres Tremante
Faculty Advisor

Table of Contents

Section **Page**

List of Figures

List of Tables

Abstract

The team will be developing the 2015 chassis and suspension for the FIU Formula SAE prototype vehicle. Several factors will be taken into account, including vehicle dynamics, chassis rigidity, vehicle component packaging and overall vehicle manufacturing and performance. This project will be split into five phases, test and validation (2014 FSAE vehicle), design, analysis, manufacturing, test and validation (2015 FSAE chassis & suspension). All decisions for design were based on all pros and cons from previous FIU FSAE testing and competitions.

Problem Statement

The purpose of this senior design project was to take improve the FIU FSAE suspension and chassis based of research, experience and testing gathers from the past two years if the FSAE program. Improvement of performance, ease of manufacturing as well as earlier assembly will provide a winning combination for the 2015 FIU FSAE team.

Motivation

The FSAE competition offers a challenging environment where engineering students practice and develop various engineering skills. Placing well in the competition occurs as a result of two categories; static testing, where design and engineering practice are judged and scored accordingly, and dynamic testing, where the actual performance of the vehicle is judged and scored. Teams that place well attain global recognition for their respective university from both the automotive industry and various even sponsors. Thus, those universities that place well attain an increase in revenues from sponsors/donations and increased relationships with these companies, which lead to an acceleration of the university's programs and an increase in job placement. Thus, the FSAE competition offers a multitude of benefits for both the students that attend and the university as a whole.

In order to place well, as previously mentioned, the vehicle must be designed with good engineering practice and must perform well. Since the event is essentially an autocross event, which favors cornering over top speed, this means having a chassis that is as light a possible while still maintaining required torsional rigidity, and a suspension system that can maximize the performance of the tires in contact with the road.

Conceptual Design (Design Alternatives)

When Designing a Formula SAE frame, many factors have to be taken into account. The frame being the main component of the prototype vehicle, the design goals for the entire car have to be set. Formula SAE vehicles are considered open-wheeled racecars. Open-wheeled race cars are usually designed from the "ground up". The design starts with interrupting of the tire data, based on tire limitations, then one can start setting realistic goals for the vehicle, including wheel base, track and overweight. Track to wheelbase ratio should be typically a 1.2 to 1.5 ratio. For quick steering response an optimal ratio of 1.3 should be achieved. The tire data also includes the slip angle of the tire, nomadic trail of the tire and optimal camber of the tire.

With all these factors studied and set, the suspension geometry can now start taking place. When designing a-arms which connect the wheel uprights to the chassis. There are many a-arm designs starting with double wishbone. Double wishbone design is almost always used for the front of the vehicle. Some advantages to the double wish done design are the flexible tuning parameters. In being flexible one can design the mounting or pickup points for minimal camber gain or whatever your suspension team goals are the vehicle dynamics and driver feedback are. Being a traditional a-arm design the forces get distributed a lot better compared to trailing arms and the actual a-arm can be designed with minimum diameter in turn being a lighter design. Some disadvantages to this design choice are the multiple factors that one has to take into account. Other a-arm designs include semi-trailing and trailing. Both are not recommended for the front of the vehicle. These both have advantages and disadvantages; few advantages are due to their simple designs and ease of manufacturing many teams choice to run these setups in the rear of their prototypes vehicles. Trailing arms do usually produce a larger moment coming from the force of the tire; the a-arm diameter and mounting points have to be able to take the loads.

Once the suspension geometry is designed for specific vehicle goals, the a-arm pickup points are given coordinates. Now the frame can start coming to life. Typically, one would want to optimize the lowest and most central center of gravity for your vehicle. To do so, map out the major components of the vehicle like the driver and engine. With the suspension pickup points, driver and engine sitting in free space connect all the components; make sure to follow the FSAE rules. Once your first iteration of the frame is complete, one can start running FEA analysis and start altering frame members to optimize weight and rigidity.

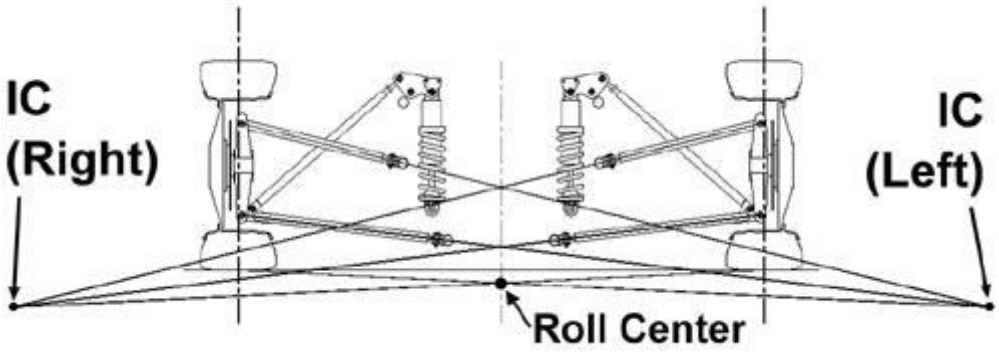

Figure 1: Calculation of the roll center based on suspension pickup points

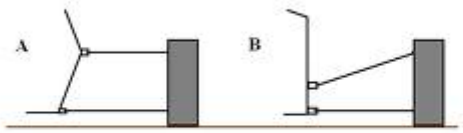

Figure 2: Difference between suspension pick up points

Figure 3: Frame design with the major components

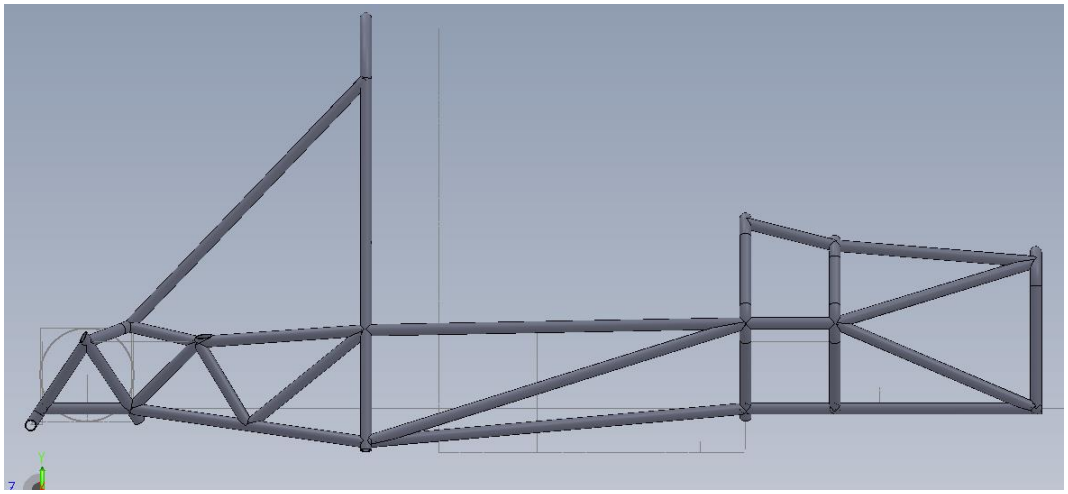

Figure 4: Side view of a preliminary design for the vehicle chassis

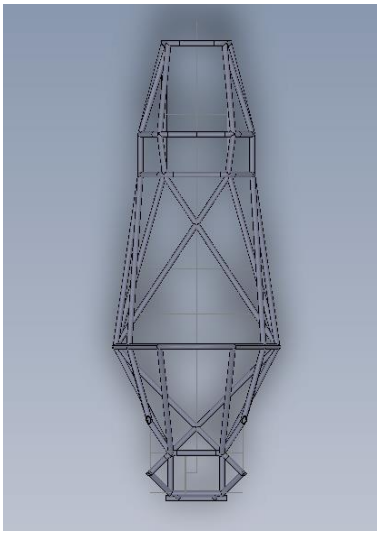

Figure 5: Top view of the same design

Once the initial design for a chassis is developed it must be analyzed. To do this several things must also occur. The application for the design must also be developed, to do this we evaluated basic translation properties of the extreme conditions we wanted the chassis to be capable of handling and made an idealized application around that worst-case scenario for the chassis to be able to withstand. This value was just an assumption since no prior cars for our school are available to conduct actual testing and providing more accurate idealized data. Once this guideline is established we must then use it in the analysis of the chassis. Due to the number of members associated with the chassis numerous equations must be calculated using Finite Element Analysis. Fortunately there are many computer programs that can make these calculations for us and establish values and images to guide our analysis and allow further development of our design. With this project we decided to utilize the simulation package for SolidWorks, which utilizes the distortional energy theory for finding stress values in the static analysis.

With using SolidWorks for the simulations we must find the best way to input our loading values and what points to classify as fixed points for our analysis. The decision to use the rear mounting points for a fixture in torsional testing was to allow as much of the chassis to experience the torsional load as possible. The simulated loading was based off where the front control arms will be mounted since that is logically where the load will be applied since the rear will be fixed since the forces applied to the chassis will be through the wheels. There were other tests that FSAE also requires which were conducted on the new chassis by fixing the appropriate points and loading the specified areas with specific loads for static testing on the main hoop, Front hoop, and side impact bar.

Primary considerations for analysis would be the deflection, stress and Factor of Safety. Deflection will change the geometry of the car when under load and have slight effects on the handling of the car. A benefit to deflection is it can help improve some aspects of handling and it provides feedback to the driver beyond just the inertial forces. The most critical aspect of the chassis design is the stresses distributed throughout the chassis. These stresses will demonstrate where critical areas are where redesign by changing angle orientation or reinforcing can help reduce the stresses and in areas where low stresses are identified that it may contain unnecessary

members or redesigning can assist in reducing weight of the chassis it can also indicate that members may be used as smaller sizes which will reduce weight but add to the complexity and possibly change the overall price. The Factor of Safety is generated from the material yield strength divided by Von Mises stress. This value provides less insight to the design capability but shows that the design meets the designer's safety criteria with a value of 1 being the absolute lowest acceptable value and the higher the value the safer the design will be.

The following images show the design and the analysis for the 2013 FIU FSAE Chassis. Some critical aspects to pay attention to are the way the chassis fits the FSAE rules with the triangular safety region for rollover protection. Another aspect to pay attention to is the relatively short wheelbase, which allows for improved handling. Within the design for the chassis the use of node-to-node connections is used to fit the rules established by FSAE. The design also incorporates triangular shaped elements allowing for a wider distribution of applied and translated stresses throughout the design of the chassis. A final aspect, which is critical in the handling of the vehicle, is the cockpit area of the chassis, which is lower than the front and rear control arm-mounting areas. This is to allow for a lower center of mass yet keeping critical suspension geometry to allow for optimal handling.

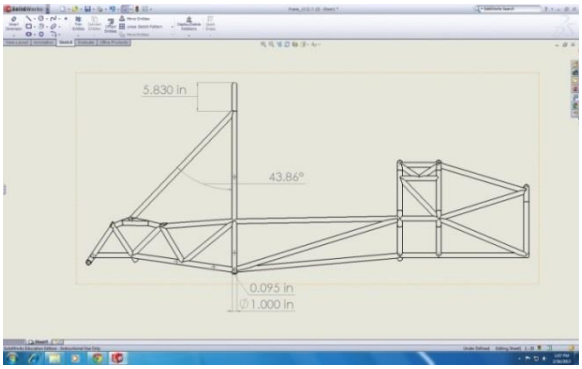

Figure 6: Chassis Drawing

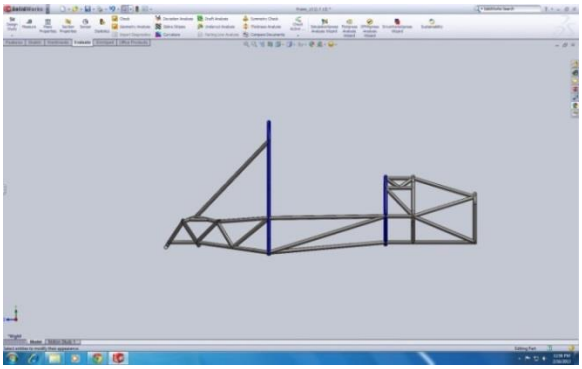

Figure 7: Chassis Side view

This image is the overhead view of the 2013 FIU FSAE chassis. From looking at this image, some primary elements to note are the middle of the chassis having wider elements, which give the design three primary benefits. The first benefit is that the operator would have more room for operating the car efficiently, providing the driver of the car more comfort and

allowing for easier entrance and exit which is critical in emergency situations. The second benefit would be a structural benefit which gives more room on chassis members allowing for better control on distributed stresses through this design and increasing potential for easily mounting required equipment. A final benefit would be safety since in a side impact the chassis will have more room to allow for the deflection of the side members to help reduce the risk of injury to the driver of the vehicle. We were able to narrow the chassis in the front and rear sections due to a small engine allowing the rear to be narrow and because of the driver's legs making the front narrow. This also allows the chassis to have a potential for lower weight since we can have options for reducing some dimensions rather than treating the chassis as a typical box configuration like what is seen on standard car chassis.

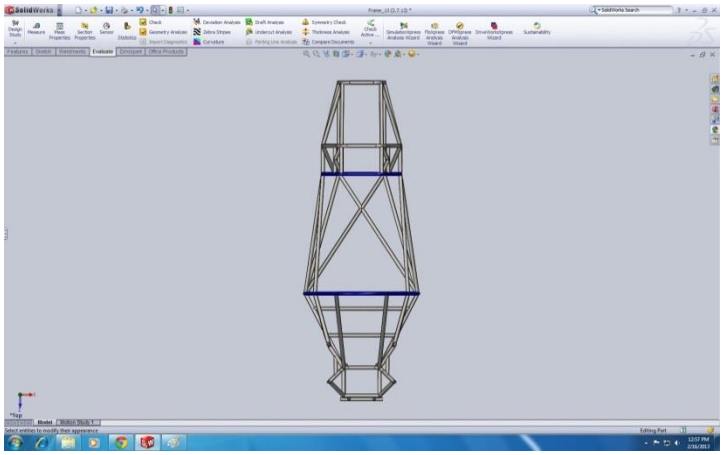

Figure 8: Top view of chassis

Viewing the chassis from the front the side impact zone can be seen on the chassis allowing another view to see the way this chassis fits the description. Due to budget constraints we also tried to minimize the number of bends in the chassis, this is due to the chassis having its cuts, bends and notching subcontracted out to a fabrication shop and the less features the shop has to create the cheaper the final cost. We can also see the front impact zone and how it is braced for head-on collision impacts with the angled member to be used as a mount for a required impact attenuator.

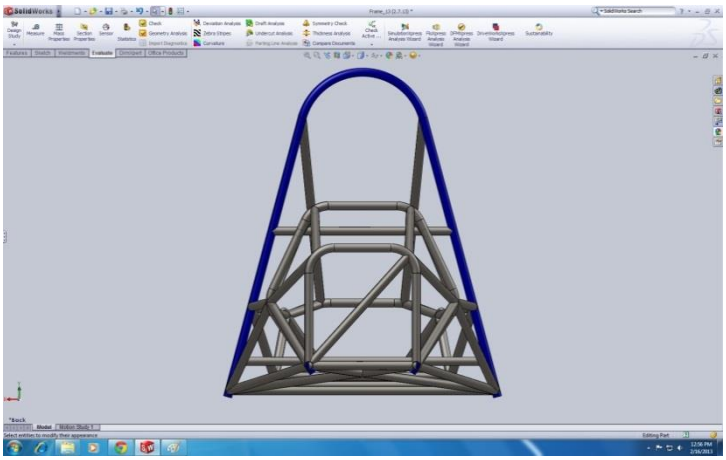

Figure 9: Chassis view from front

The rear view of the chassis shows how triangular orientation of the members in the rear of the chassis occurs and the attempt to maximize the number of load baring members to help make sure each element of the chassis serves a purpose.

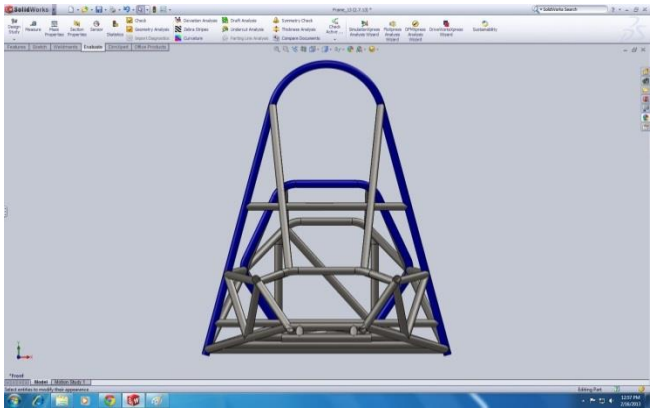

Figure 10: Chassis view from rear

We are including the following two images to help show the design elements previously discussed in this analysis. The image on the right also estimates a weight of the final chassis being 72.28LBS.

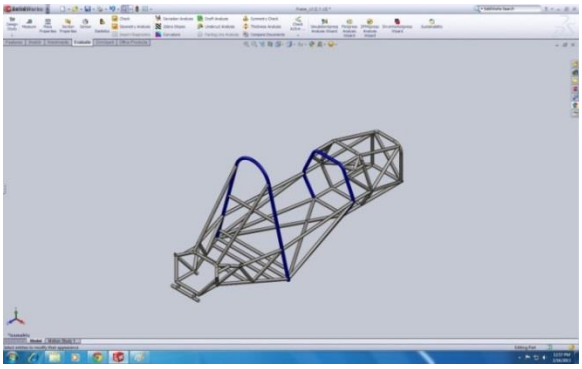

Figure 11: Isometric view of chassis

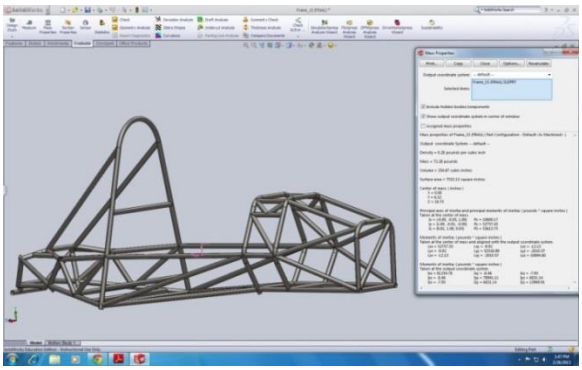

Figure 12: Mass properties of chassis

The following images show a front impact test of the chassis. Placing a dynamic load outlined in the 2013 FSAE rules of 150kN on the front of the chassis where an impact will occur does this test. By viewing these images there are many things that can be seen which would include displacement of various members in the design, the way the chassis distorts showing driver safety potential from a controlled folding of the chassis rather than a crushing effect. This controlled folding is due to the triangular orientation of the members within the chassis. And the triangular segment that is located under the floor pan of the car where the driver will be sitting.

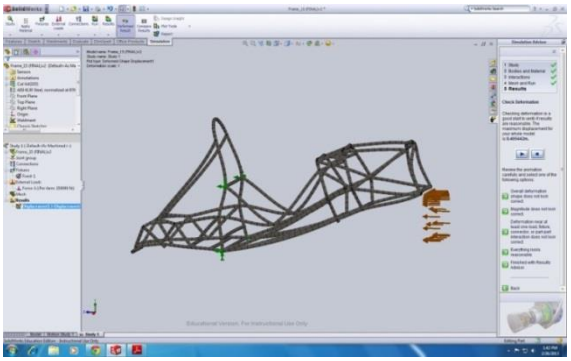

Figure 13: Front impact load on chassis

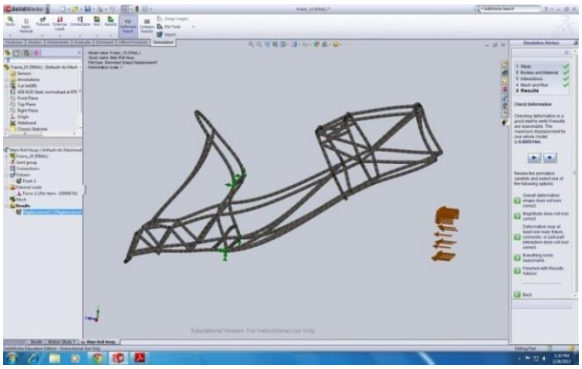

Figure 14: Front impact deformation of chassis

The following images are provided as outlined in the 2013 FSAE rules with a static load placed in specific magnitudes and specific directions on the front and main hoops of the chassis along with a static load on the side impact beams of the chassis. These members are crucial to see how they deform under load and how they distribute stress throughout the system for understanding their ability to provide driver safety, which is critical when the potential loss of human life is involved in an engineer's product. The reason for a static load is not exactly known, since a dynamic load would better simulate an accident but the general description of static loads can provide insight to the dynamic potential of these members.

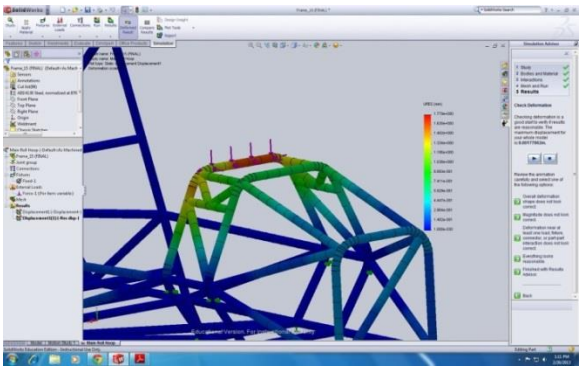

Figure 15: Load on front roll hoop 1

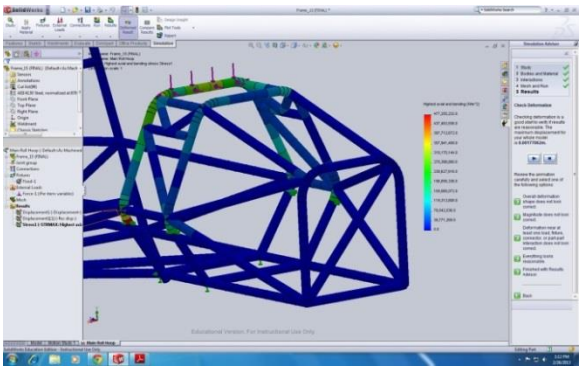

Figure 16: Load on front roll hoop 2

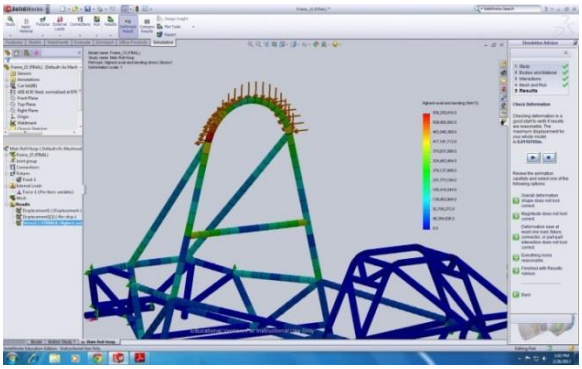

Figure 17: Load on main roll hoop 1

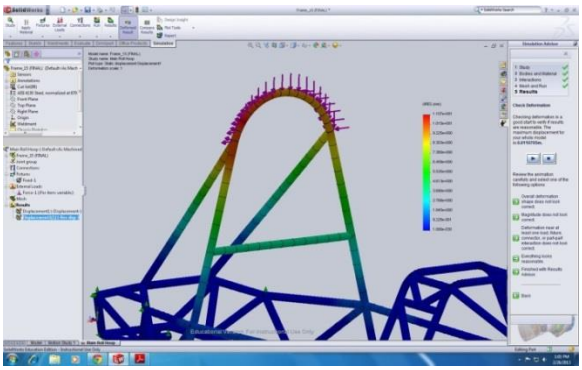

Figure 18: Load on main roll hoop 2

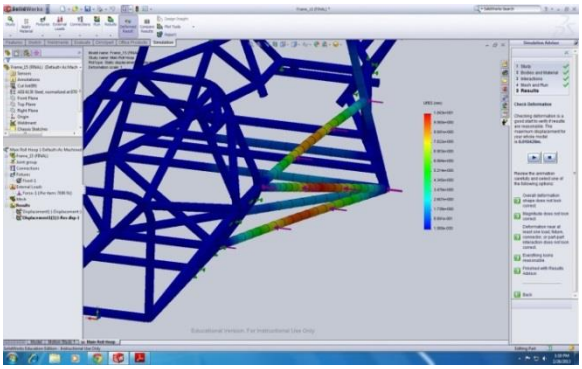

Figure 19: Load on side impact structure 1

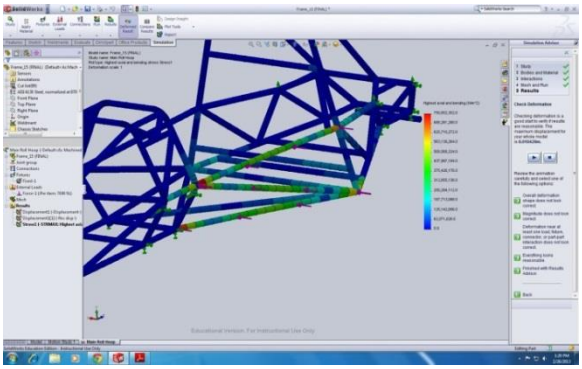

Figure 20: Load on side impact 2

To demonstrate the structural integrity of the chassis we place a torsional load on the front control arms and fix where the rear control arms will be mounted. This load is created by a positive static load on one side of the chassis and negative on the opposite side which will translate to torsion. This analysis we found to be the most critical since it defines the reaction of every member throughout our chassis in cornering which is vital in any sort of racing that incorporates turning or extremely high torques on the chassis. Many things can be seen with this analysis that is critical in our design and in future revisions. One of the first things to notice is the stress developed through each member. These stresses when combined with the Yield strength show the Factor of Safety through the design. This is defined as (Yield Strength/Von Mises Stress = Factor of Safety). You can also generate this plot separately on SolidWorks,

which is shown in the analysis of the 2012 FIU FSAE Chassis. The extremely low and extremely high values of stresses in the design show where design revisions may be beneficial. In cases with high stresses reinforcing the area or altering the angles of members may translate the stresses better throughout the entire structure, which will increase operator safety. By altering areas where low stresses are found we can remove members that will translate those stresses, which will reduce chassis weight.

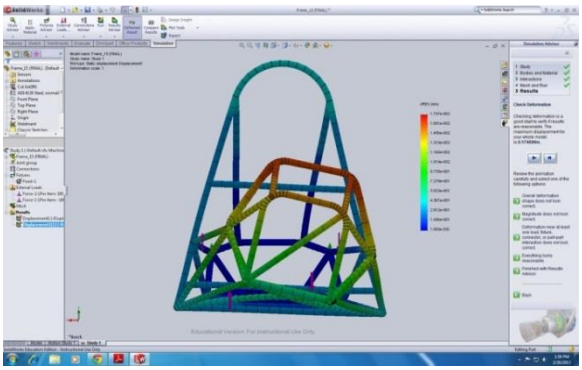

Figure 21: Torsional load on chassis 1

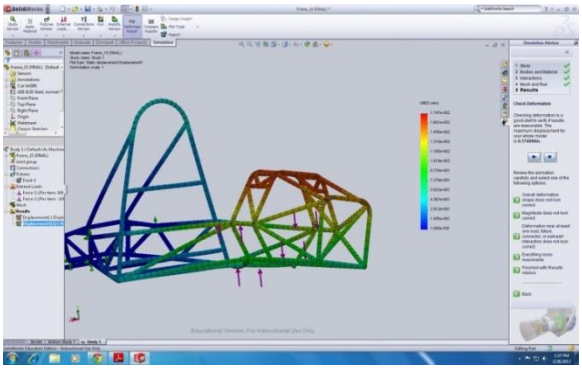

Figure 22: Torsional load on chassis 2

Proposed Design

Chassis

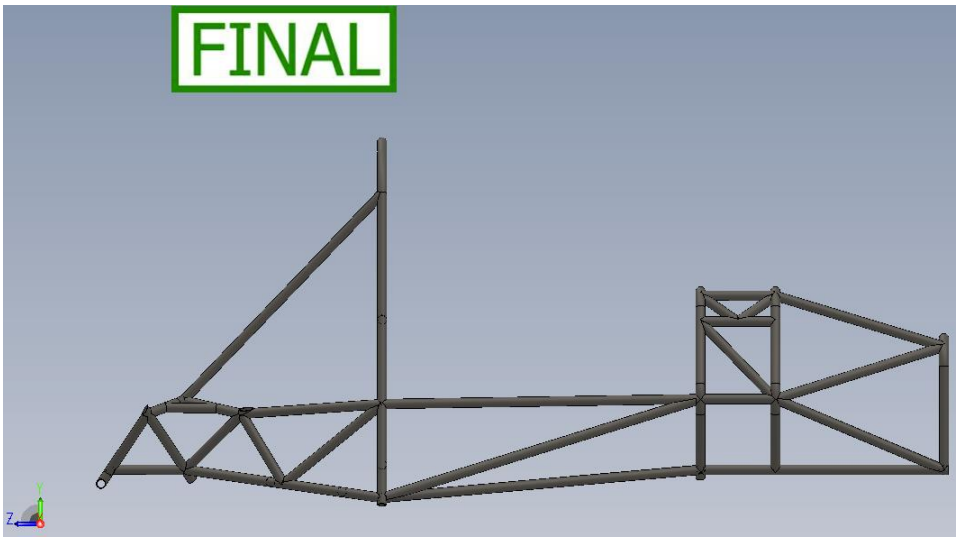

Figure 23: Final chassis design side

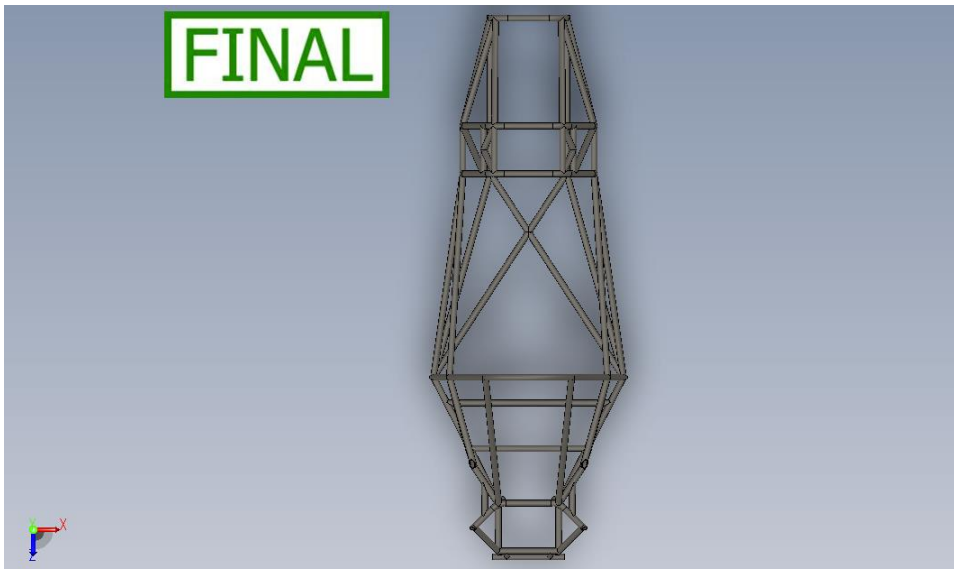

Figure 24: Final chassis design top

Table 1: Chassis proposed cost report

University:	Florida Internatioanl Univeristy
Car #:	20
System:	Chassis
Technical Lead:	Osvaldo Fernandez

Part	Reason	Specifications	Cost per Unit	Size of Unit	# of Units	Total Cost
4130 Alloy Steel	Frame	Round 1.0" (OD) X 0.065" (WT)	$0.32	1 in	1404	$449.28
	Roll Hoop	Round 1.0" X 0.095"	$0.55	1 in	240	$132.00
6061-T6 Aluminum	Firewall	0.125", 12" X 12", 1.76lbs per ft^3	$13.01	144 in^2	2	$26.02
	Floor	0.125", 12" X 12", 1.76lbs per ft^2	$13.01	144 in^2	5	$65.05
End Mills	Notching	Mill Dia: 1", Shank Dia: 3/4", Lg of Cut: 1 7/8"	$42.07	1 end mill	3	$126.21
E70S2	Filler Rod	E70S-2	$3.22	1lb	5	$16.10
Tungsten Tips	Tungsten Tips	2% Type, Ceriated, Color Code: Orange	$14.48	1 pk (10)	3	$43.44
Cartesian CNC	Pipe notching, Bending, & Raw materials		$2,500	1 FSAE Vehicle	1	$2,500
CRD Laser Tube Cutting	Pipe notching, and Bending		$415	1 FSAE Vehicle	1	$415

Grand Total w/o outsourced pipe notching	$858.10	24hrs of labor for notching and bending
Grand Total w/ Cartesian	$2,650.61	
Grand Total w/ CRD	$1,146.89	CRD does not supply raw materials

Teams on the FSAE forum claim that Cartesian has reduced their sponsorship assitance by 50%, and have increased toral cost by almost $1000. The cost estimate for Cartesian above does not include this influx in price.

The chassis was designed with driver ergonomics and weight reduction in mind. Following up on our engine choice, the car needed to be as lightweight as possible to effectively benefit from the single cylinder motor. The chassis is a completely tubular space frame fabricated with chromoly steel round tubing. Design of the chassis began with the suspension pick up points. The rear legs of the front suspension arms will be affixed to the front roll hoop, 8 inches forward there is an identical hoop of 0.065-inch wall thickness where the front arms of the suspension will mount. Theses hoops were designed to provide maximum driver leg room while maintaining our desired track length. The front bulkhead was designed to the exterior dimensions of the standard FSAE impact attenuator. The distances between the front bulkhead, the front roll hoop, and the main roll hoop were decided using a driver ergonomics rig. The width of the chassis at the bottom of the main roll hoop was chosen to provide maximum room from engine and electrical components as well as to reduce complexity of the chassis in this area by limiting the number of bends in the main hoop. Our designs were made so that the engine can be inserted from the right side of the chassis, between the main roll hoop and the main roll hoop supports. The mounting system, which consists of lateral bars stretching the width of the chassis with tabs mounting to the engine, was kept simple to reduce complexity of design, improve manufacturability, and reduce overall cost. The engine has been offset 1.5 inches to the right to allow for better fitment of the differential; all engine components will be mounted on the left to balance the weight of the engine. When designing the chassis, the decision was made to minimalize the rear box for ease of access and servicing of drivetrain components as well as to reduce weight of the chassis. The section of bent tubing mounted to the rearward, upper suspension mount is placed to distribute the load of the suspension as well as to provide a location for mounting of the shocks, and chain guard. The jacking point was positioned slightly rearward of the last frame member so it would not interfere with the suspension during travel. Overall the chassis weighs approximately 73 lbs., which is just shy of our 70 lbs. goal.

Suspension

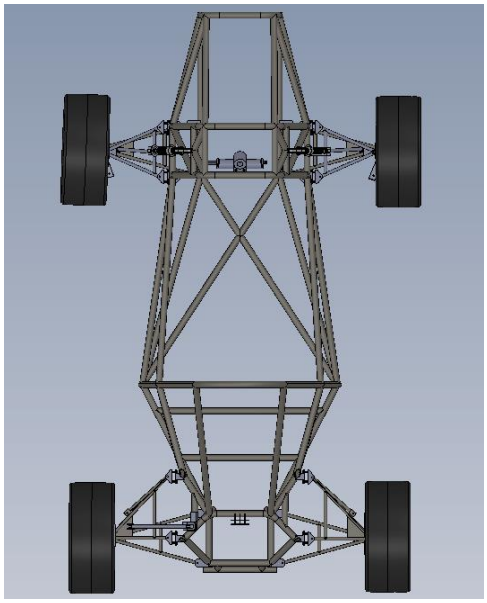

Figure 25: Suspension and tire mounted to chassis

The suspension system for this year's car has been completely redesigned from last year. The biggest emphasis around the design was to maintain low weight. Each corner of the car is independently suspended and incorporates a push rod system.

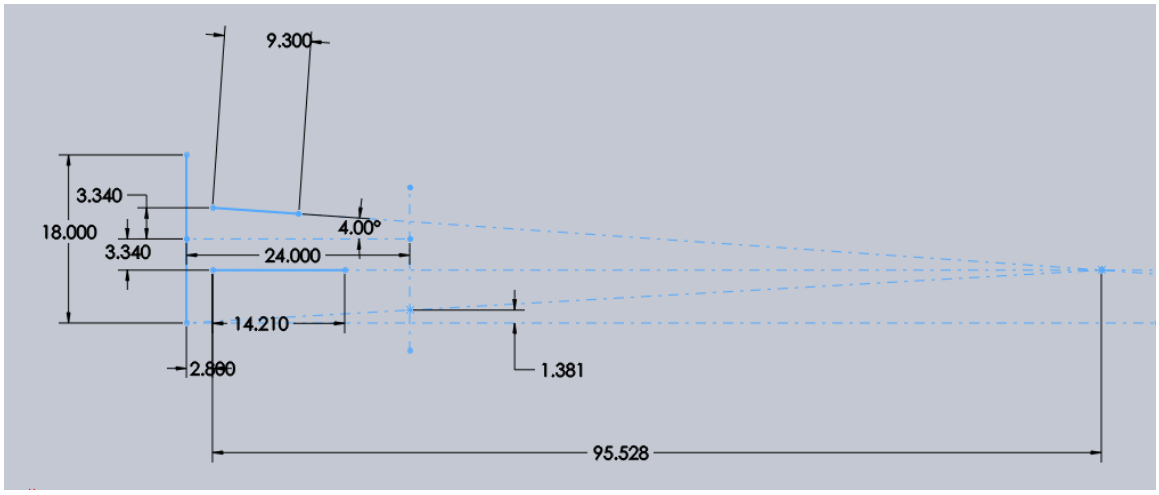

Figure 26: Proposed suspension geometry

The suspension upright has been designed out of T6-6061 aluminum to maintain low weight while maintaining strength and easy machinability. All designs were minimalistic in nature in order to decrease weight, but more importantly for packaging purposes. Improvements have also been done in the area of a fixed kingpin angle and caster already implemented into the upright. The spindle has multiple steps in size. This is to increase the surface area that is pressed into the upright. This also allows for smaller bearings, which in turn reduces the overall weight

of the system. The hub is an essential component of the suspension as it's the main un-sprung rotating component. It has been designed using T6-6061 aluminum, which is lighter than other metals thus requiring less torque for acceleration. Two bearings are used per wheel in order to distribute the load on the spindle more evenly.

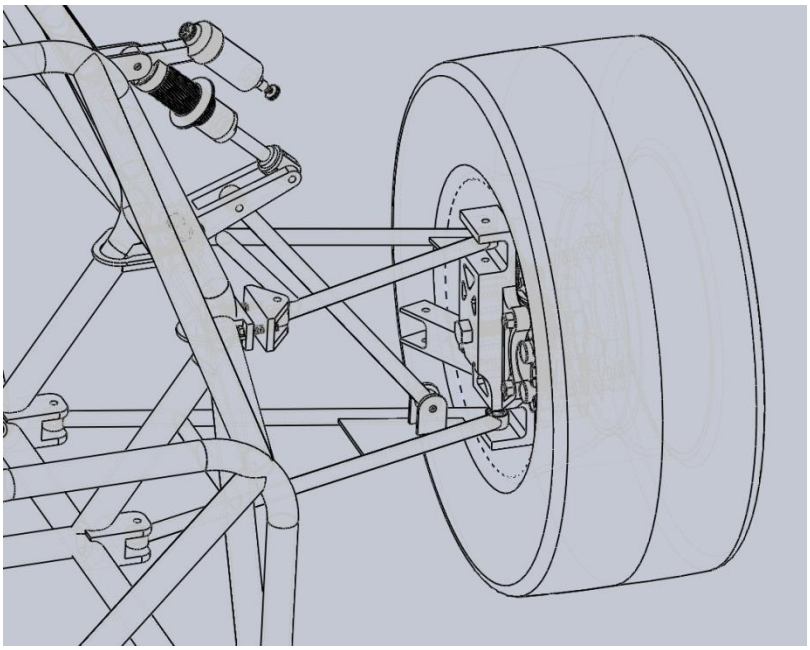

Figure 27: Front left wheel and tire package

The suspension geometry has been meticulously designed to take full advantage of the tires that will be used and to maintain a low roll center for the car. The arms have been designed with spherical bearings for all attachment points. This maintains all forces transferred in line with the bearings, eliminating unnecessary moments. The suspension has been designed for ease of tuning. The most significant improvement to the suspension is the ability to adjust the camber quickly by placing shims at the point where the A-arms meet the chassis. The reason for this design was to be able to adjust the camber while maintaining a constant king pin angle.

Suspension Geometry Camber analysis W/O Body Roll

- Various ratios of A-Arm length were looked at with a varying degree of initial camber and top A-Arm angle, while maintaining the bottom A-Arm parallel to the horizontal.

Only ratio Comparison at 0 Static Camber
Equal Distance

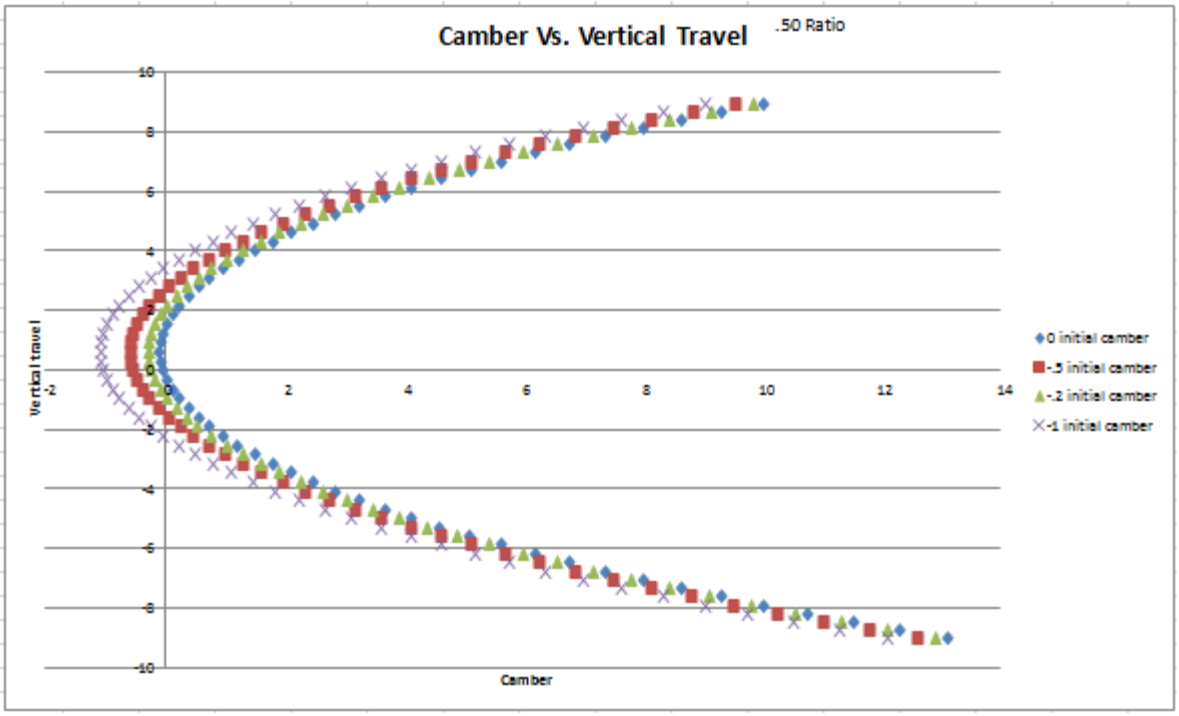

Figure 28: Camber VS vertical travel .50 ratio

- Negative camber is better than positive camber, 0 is optimum.
- Minimum Suspension travel by the rules is 2 in travel.
- Keeping to the minimum required shows at full compression of about 2.19 in of vertical travel has a +.22 camber, Close to 0, but + nonetheless. Negative is preferred over positive.
- The inside tire, although it has reduced grip because of weight transfer, its not beneficial to lose further grip with +.95 deg camber.
- Short amount of suspension travel, positive camber at both extremes of the travel, Negative or close to 0 camber almost only with no suspension travel.
- Final Score of 4 (1 optimum, 5 worse)

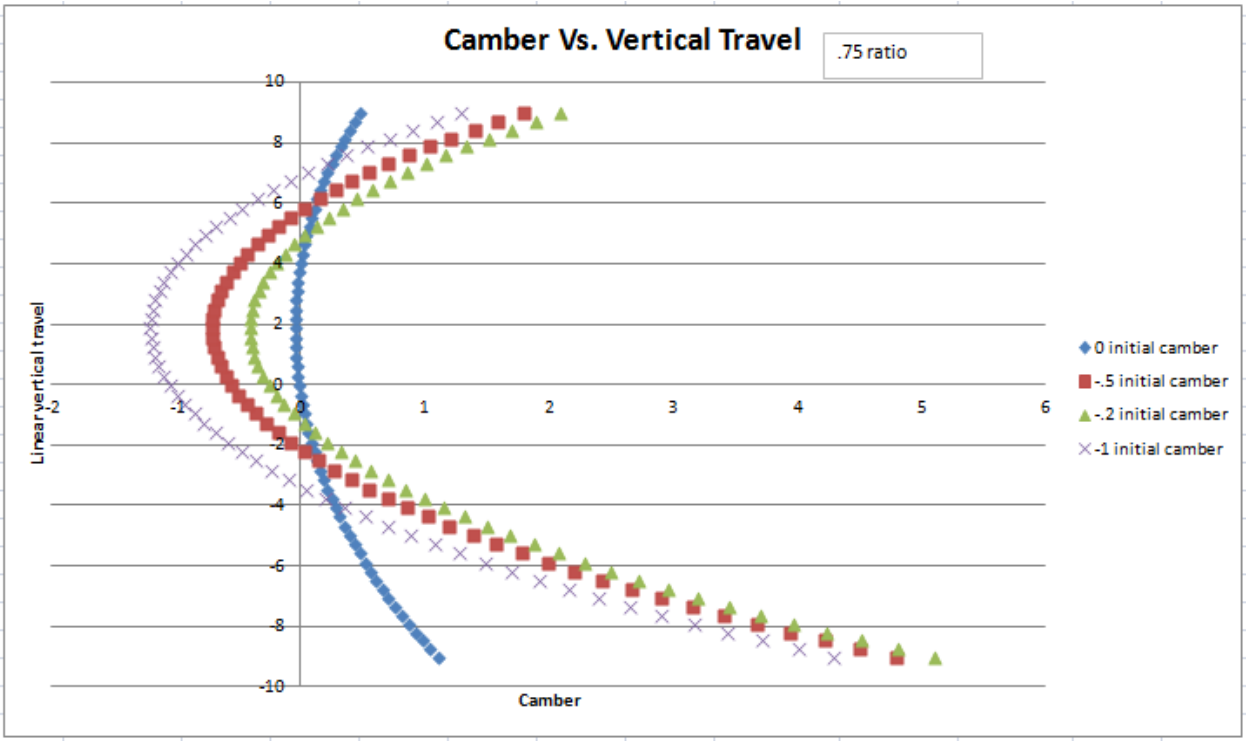

Figure 29: Camber VS vertical travel .75 ratio

- As close to 0 deg of camber is observed at 4 in of upward travel, it a good amount of travel to account for bumps.
- Formula 1 cars run 0 droop travel, but since this is not a formula 1 car keeping a max of 2 in of droop will give a +.48 of camber, grip is reduced but not extremely.
- Good amount of suspension travel with decent amount of camber change.
- Final Score of 2 (1 optimum, 5 Worse).

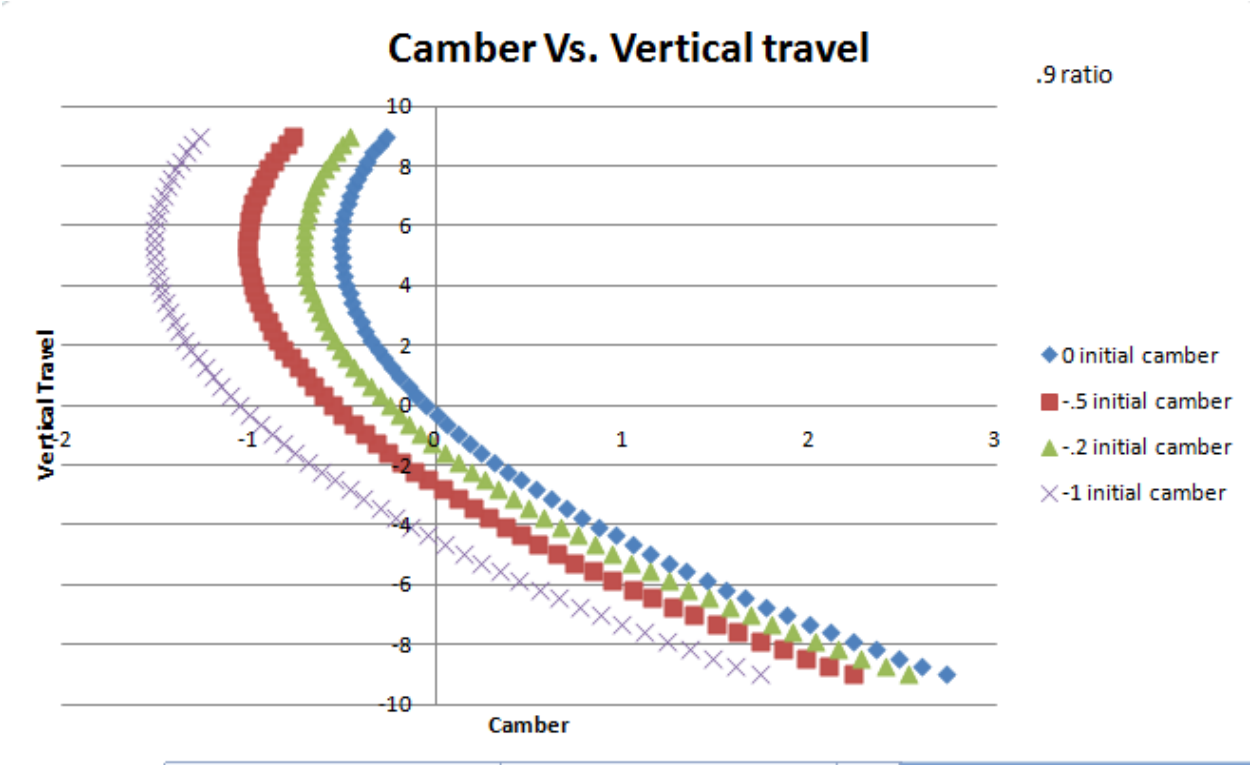

Figure 30: Camber VS vertical travel .9 ratio

- 0 deg is seen at a max travel of 0, no travel for the suspension is unacceptable.
- Following the upward vertical travel, the camber becomes increasingly negative until about 5.26 in of travel, which later camber begins to decrease to 0. Far too much suspension travel to reach 0 deg camber. Way past bump stop.
- Negative camber is better than a positive, but this ratio is by no means optimum.
- Final Score of 5 (1-Optimum, 5 worse).

Conclusion:

- .75 ratio seems to be best suited, analyzed at 0 static camber and no body roll accounted.

Literature Survey

An FSAE chassis and suspension design is done yearly by every team that intends to compete. Thus, there are various design types that has been explored that offer its own benefits and costs. All of these designs follow the mandated specification given by the competition rules, yet each of them fall are unique. For suspension design, most teams employ a double wishbone suspension, using either a push-rod or a pull-rod system to actuate the rocker for the shock and spring assembly. Pull rods are more advantageous for a lower nosed vehicle, allowing for a lower packaging of the suspension assembly and therefore a lower center of gravity, thus increasing vehicle performance. But, the disadvantage is that due to the required suspension geometry for the pull-rod, and the fact that the nose of the vehicle is made lower, upsetting aerodynamics. Thus, the choice between push rod vs. pull rod largely depends on the packaging and aerodynamic requirements of the vehicle.

In terms of the chassis itself, there are a multitude of construction types allowed in the competition rules. Each with their own set of advantages and disadvantages; they will be further explored below.

Carbon Fiber Monocoque

A carbon fiber monocoque is used by teams with extensive amounts of research and resources into the development of carbon fiber structures. Carbon fiber is a composite that possesses twice the strength of steel, yet is five times lighter, making it the perfect choice for a chassis. Many of the top tier teams, such as those from Oregon State University and Tu Graz, and even in certain classes of motorsports such as Formula 1, employ this chassis design, taking advantage of its light weight and relative strength. A monocoque is essentially a structural skin, where the body of the vehicle supports the external loading that is being applied from the suspension, brakes, engine, etc. Since the monocoque is also the external body of the vehicle, it is also made to be aerodynamic. The chassis also must be crash tested and proven to satisfy minimum safety standards set by the design judges.

Despite the advantages of this chassis design, there is one glaring drawback; it is very expensive in both cost and time to both design and manufacture. Thus at this current stage, a carbon fiber monocoque is not a feasible design choice for this project.

Aluminum Space Frame/monocoque

Aluminum has been successfully used by various universities in the FSAE competition. As a space frame, aluminum is not a likely candidate; as per the rules any aluminum tube member must be made thicker than a comparable steel member. This, combined with the fact that aluminum is not as rigid as steel and is much tougher to weld reliably, makes it a poor choice for a space frame.

Many teams, such as Cardiff University, who decide to use aluminum do so in a monocoque form. Similar to a carbon fiber monocoque, the aluminum frame is also considered the external body of the vehicle. But, an aluminum monocoque does not offer as much weight

savings as a carbon fiber one. Thus, for the purpose of this project, the extra expense needed for an aluminum space frame is not justified by the benefits expected.

Steel Space frame

The steel space frame is the standard among FSAE team. Although heavier than other chassis design, it offers ease of use in material machinability, welding, and cost. Plenty of other motorsport classes use this type of frame, such as GT and Touring car racing. For teams who are new to the FSAE competition and who may not have a myriad of manufacturing resources, this chassis is the perfect starting point for the first few prototypes. Thus for our project, a steel space frame is the most logical choice.

Timeline and Responsibilities

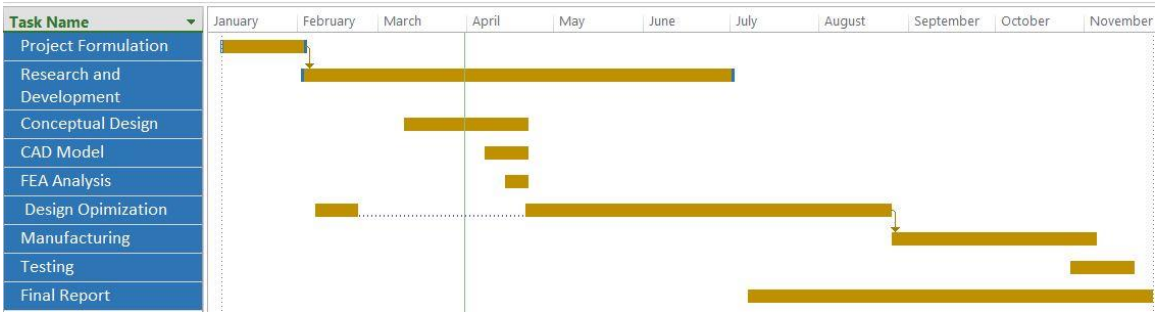

Responsibilities	Design Suspension	Design Chassis	Manufacturing	Analysis
Christian Ramos				
Osvaldo Fernandez				
Alex Diaz				
Ricardo Gonzalez				

Analytical Analysis

Tire Data Analysis

As mentioned before, the design of an open-wheeled racer begins from the tires. This is due to the fact that all of the forces and moments that the vehicle experiences is reacted by the road through the four contact patches of the car. It should be noted that different tire compound produce different lateral and longitudinal forces based upon the camber and toe angles of the tire, and it is due to these characteristics that the suspension geometry is designed; in order to best maximize the tire compound. Thus, accurately analyzing and modeling the tires is crucial to attaining the desired dynamics of the vehicle.

The raw tire data is usually done and provided by the manufacturers, but for FSAE purposes the data for the various tires available for the team are provided by Calspan Tire Research Facility. This raw data is acquired by mounting the tire on a flat belt test machine with 120 grit paper and a test velocity of 25 mph. The data is collected in sweeps, and the loading of the tire and the camber and slip angles are varied and the various tire parameters such as the lateral and longitudinal forces, aligning torque, overturning moment and the loaded and effective radius of the tires are measured.

In its raw form, tire data does not offer much in terms of modeling and predicting tire characteristics. The data is usually plotted on various graphs, where certain tire characteristics can be observed and a preliminary analysis can be made of the tires. The problem lies in the fact that tires characteristics vary greatly when exposed to different conditions such as road surfaces and temperatures. Thus this method is not entirely accurate for analyzing and simulating how tires will react to future conditions.

To overcome this limitation the automotive industry uses a mathematical model of the tire called the Pacejka Magic Formula. This formula characterizes the tire by a set of 10-20 coefficients for each force or moment the tire can produce. The coefficients themselves are found using the raw testing data of the tire. The raw data is inputted into a tire modeling software such as MF-Tool, which plots the experimental data along with a curve fit. The curve fit is used to find the needed coefficients of the tire. A sample output of the tire file is included Appendix B for reference. The equation uses this formula to determine the resultant lateral and longitudinal force along with the aligning and overturning moment that the tire is producing for a given load, slip angle camber angle and slip ratio. The general equation for the Pacejka formula is:

$$F(x) = D\cos[C\ \arctan\{Bx - \mathrm{E}(\mathrm{Bx} - \arctan(Bx))\}]$$

Where F(x) is the force or moment occurring from a slip parameter x, which is either the slip ratio or the slip angle. The coefficients B, C, D, and E are fitting constants that are calculated from the 10-20 Pacejka coefficients that are characterized by the tire using additional formulas found in Appendix C.

This Pacejka model will be created using MatLAB, where inputs can be fed into the formula and the reaction from the tires can be outputted and analyzed. This MatLAB model also allows various vehicle simulating software, such as ADAMS and LapSim, more effectively, thus

allowing for more accurate simulations of the vehicle as a whole and a better attainment of the desired vehicle performance.

Chassis and Suspension

The following are the formulae used throughout the project. Some of the variables can be referenced to the nomenclature section for further clarification if necessary.

$$Motion\ Ratio\ (MR) = \frac{Spring\ Travel}{Wheel\ Travel} = \frac{\Delta x_s}{\Delta x_w}$$

$$Wheel\ Rate\ (WR) = (Spring\ Rate)(MR)^2(Spring\ Angle\ Correction) = (k_s)(MR)^2(cos\theta)$$

$$Spring\ Rate = k_s = \frac{Gd^4}{8nD^3}\ or\ F_s = k\Delta x$$

G=modulus of rigidity
d=wire diameter
n=# of active coils
D=coil diameter

$$Torque\ required\ to\ rotate\ chassis\ about\ roll\ axis = T = \frac{t^2}{2}k\theta$$

t=spring rate
IF (WR) is used for k, then t is equal to track width
k=spring rate OR wheel rate
θ=angular displacement

$$Roll\ Stiffness = k_{\varphi} = \frac{T}{\theta} = \frac{t^2}{2}k$$

$$Conversion\ factors\ for\ Roll\ Stiffness = \frac{t^2}{2}k\left[\frac{N \cdot m}{57.3 \cdot °}\right] = \frac{t^2}{2}k\left[\frac{lb \cdot ft}{57.3 \cdot ° \cdot 12}\right]$$

$$Grip = \frac{Lateral\ force}{Normal\ force} = Coefficient\ of\ friction$$

$$Centrifugal\ Force = \frac{(mass)(g)(cornering\ speed)^2}{(14.97)(corner\ radius)}$$

$$Lateral\ Acceleration = \frac{Centrifugal\ Force}{(mass)(g)}$$

$$Front/Rear\ Weight\ Distribution = \frac{\%\ Front}{\%\ Rear}$$

$$\%\ Wt.Front\ Tire = \frac{100 \cdot R}{WB}$$

$$\%\, Wt.\, Rear\ Tire = \frac{100 \cdot F}{WB}$$

WB=wheel base

Optimal Suspension Parameters:
Wheel Base: 60” (smallest allowable WB)

$$\frac{Track\ Width}{Wheel\ Base} = 1.3$$

$$Average\ Track = \frac{Front\ Track + Rear\ Track}{2} = 46"$$

$$Rear\ Track = (0.98) Front\ Track$$

$$Front\ Track = 46.5" \approx 47"$$
$$Rear\ Track = 46.06" \approx 45”$$

Reason for choosing 45 inches: To give more clearance for the rear of the vehicle while weaving through cones during the competition.

Major Components

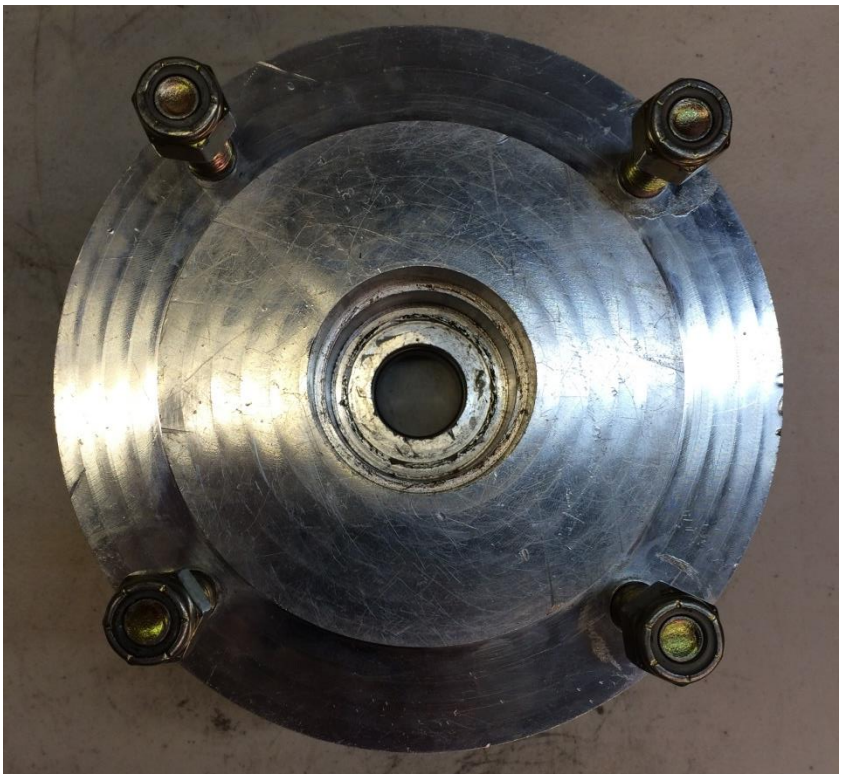

Figure 31: Wheel hub – Front view

Figure 32: Wheel hub – Rear view with brake rotors

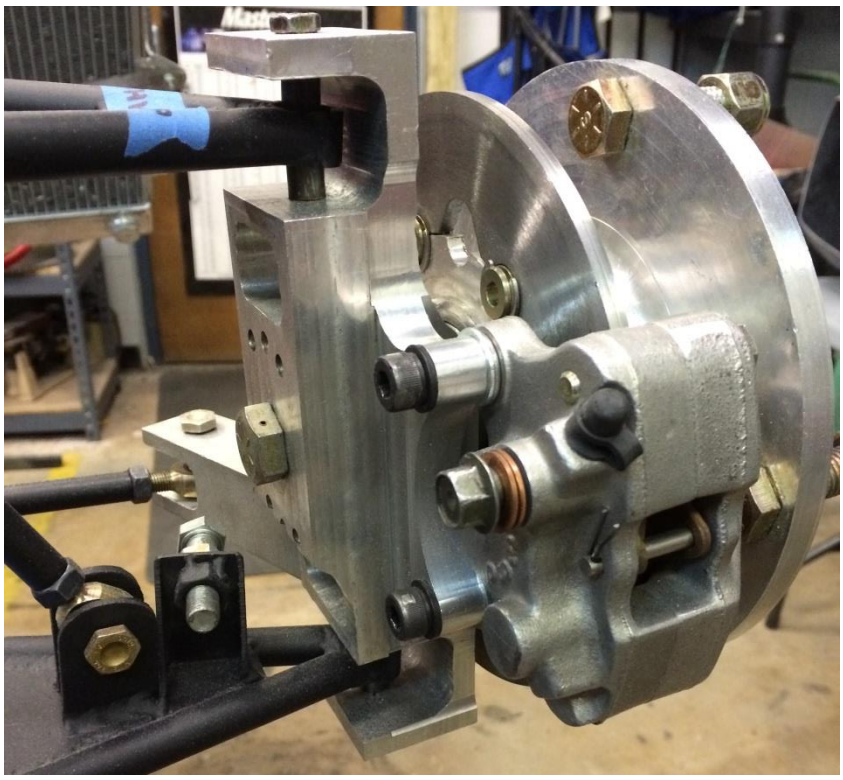

Figure 33: Hub/Upright Assembly with brake calipers

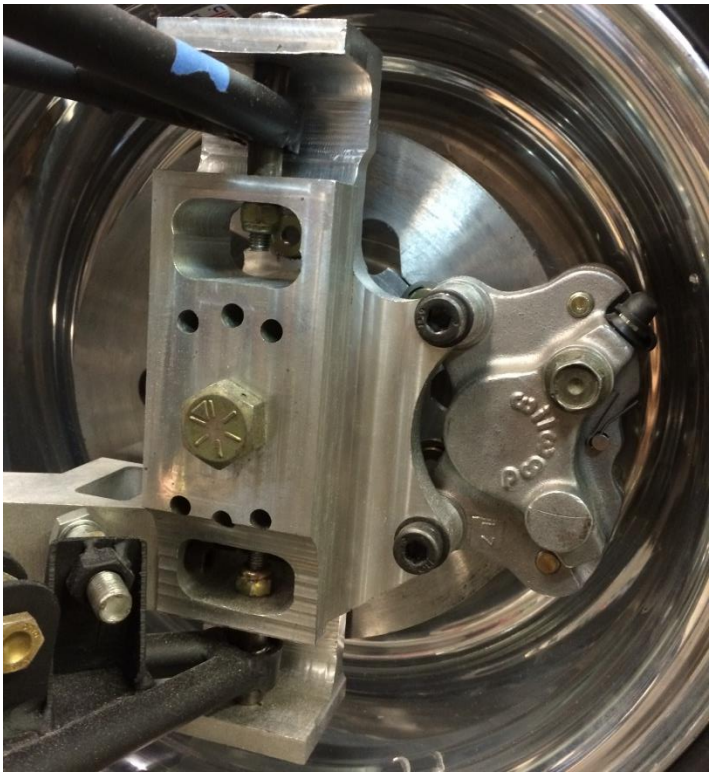

Figure 34: Hub/Upright assembly with wheel

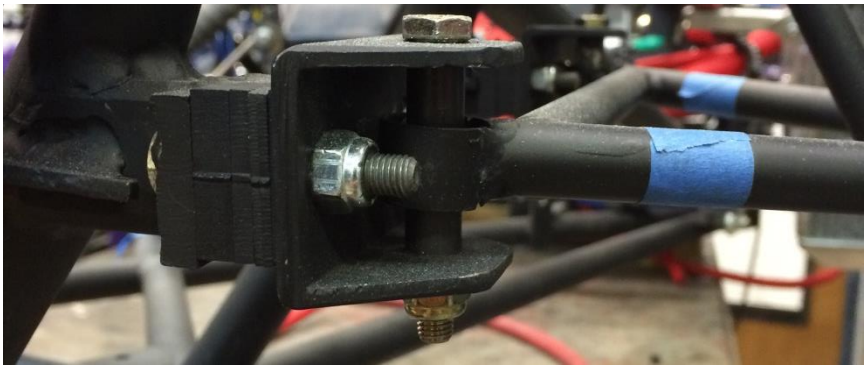

Figure 35: suspension pick up point top

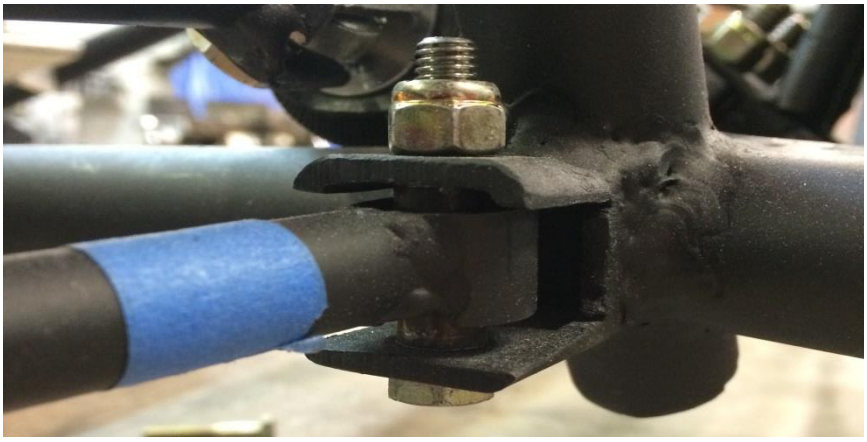

Figure 36: Suspension pick up point bottom

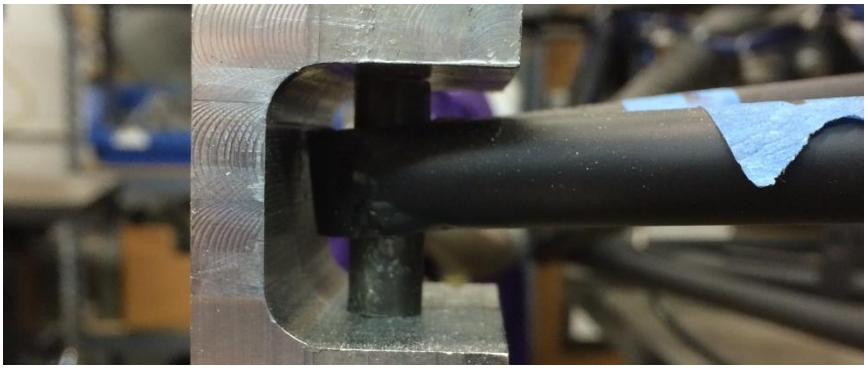

Figure 37: Top upright A-Arm mount

Figure 38: Front left suspension geometry

Figure 39: Front left suspension geometry with wheel

Figure 40: Rear suspension geometry

Cost Analysis

Table 2: Frame cost breakdown

Description	Unit Cost	Quantity	Material Cost	Process Cost	Fastener Cost	Total Cost
Frame	$512.27	1		$512.27		$512.27
Brackets	$1.63	15	$0.68	$0.95		$24.45
Tube Cuts/Bends	$247.50	1	$74.22	$173.27		$247.50
Tube End Preparations	$279.00	1	$279.00			$279.00
Shifter	$39.53	1	$37.91	$0.93	$0.69	$39.53
Linkage	$29.32	2	$5.96	$23.35		$58.63
Shifter Cable / Linkage	$30.16	1	$30.00	$0.16		$30.16
Body	$4,350.58	1	$3,573.60	$758.98	$18.00	$4,350.58
Pedals	$170.56	1	$28.19	$142.37		$170.56
Total			$4,029.57	$1,612.29	$18.69	$5,712.68

Table 3: Suspension cost breakdown

Suspension Cost						
Component	Unit Cost	Quantity	Material Cost	Process Cost	Fastener Cost	Total Cost
Bell Cranks	$69.36	$4.00	$5.66	$63.70		$277.44
Spindle Nut	$6.30	$1.00	$6.30			$6.30
Springs & Damper	$204.08	$4.00	$200.00	$2.96	$1.12	$816.32
Suspension Mechanism	$18.92	$1.00		$15.40	$3.52	$18.92
Front Left Lower A-Arm	$33.32	$1.00	$4.23	$29.09		$33.32
Push rod bracket	$28.63	$1.00	$0.05	$28.58		$28.63
Rod end bearing cup	$4.17	$1.00	$2.46	$1.71		$4.17
Sheet metal support	$22.38	$1.00	$0.06	$22.32		$22.38
Front Left Upper A-Arm	$22.74	$1.00	$18.63	$3.54	$0.57	$22.74
Pushrod	$14.06	$1.00	$13.28	$0.70	$0.08	$14.06
Structure	$32.18	$1.00	$4.23	$27.95		$32.18
Sheet metal support	$8.36	$1.00	$0.06	$8.30		$8.36
Rod end bearing cup	$4.17	$1.00	$2.46	$1.71		$4.17
Front Right Lower A-arm	$25.82	$1.00	$18.63	$6.24	$0.95	$25.82
Push rod bracket	$28.63	$1.00	$0.05	$28.58		$28.63
Rod end bearing cup	$4.17	$1.00	$2.46	$1.71		$4.17
Sheet metal support	$22.38	$1.00	$0.06	$22.32		$22.38
Structure	$33.32	$1.00	$4.23	$29.09		$33.32
Front Right Upper A-arm	$22.17	$1.00	$18.63	$3.54		$22.17
Pushrod	$14.06	$1.00	$13.28	$0.70	$0.08	$14.06
Structure	$32.18	$1.00	$4.23	$27.95		$32.18
Rod end bearing cup	$4.17	$1.00	$2.46	$1.71		$4.17

Sheet metal support	$8.36	$1.00	$0.06	$8.30		$8.36
Rear Left lower A-arm	$67.45	$1.00	$63.34	$3.54	$0.57	$67.45
Rear Left upper A-arm	$170.56	$1.00	$163.37	$6.24	$0.95	$170.56
Rear Right lower A-arm	$67.45	$1.00	$63.34	$3.54	$0.57	$67.45
Rear Right upper A-arm	$170.56	$1.00	$163.37	$6.24	$0.95	$170.56
Rear left pushrod	$14.06	$1.00	$13.28	$0.70	$0.08	$14.06
Rear right pushrod	$14.06	$1.00	$13.28	$0.70	$0.08	$14.06
Front left upright	$3.81	$1.00		$3.22	$0.59	$3.81
Front left upright spindle	$2.84	$1.00	$0.59	$2.25		$2.84
Front left upright steering linkage	$3.88	$1.00	$0.84	$3.04		$3.88
Front left upright structure	$21.25	$1.00	$11.95	$9.30		$21.25
Front right upright	$3.81	$1.00	$3.22	$0.59		$3.81
Front right upright spindle	$2.84	$1.00	$0.59	$2.25		$2.84
Front right upright steering linkage	$3.88	$1.00	$0.84	$3.04		$3.88
Front right upright structure	$21.25	$1.00	$11.95	$9.30		$21.25
Rear left upright	$77.75	$1.00	$76.81	$0.94		$77.75
Rear left upright structure	$21.81	$1.00	$11.95	$9.86		$21.81
Rear right upright	$77.75	$1.00	$76.81	$0.94		$77.75
Rear right upright structure	$21.82	$1.00	$11.96	$9.86		$21.82
Total			$1,625.98	$611.63	$13.47	$2,251.08

Table 4: Steering cost breakdown

Steering Costing						
Steering Rack & Pinion	$100.32	$1.00	$48.37	$50.84	$1.11	$100.32
Steering Shaft	$72.35	$1.00	$53.18	$18.74	$0.43	$72.35
Steering Wheel	$70.14	$1.00	$54.82	$15.32		$70.14
Total			$12,545.13	$7,530.65	$142.47	$242.81

Prototype System Description

There will be two prototypes involved with the design. The 2014 Prototype SAE car (prototype 1) will be a test bench for prototype 2. This prototype will be a running and driving vehicle, from which all the vehicle dynamics adjustments and goals will be verified. This system includes the chassis and suspension with all other vehicle system components such as braking system, power train and drive train systems, aero package and full electrical package.

A second prototype will be built in the last phase of the project. This prototype will include the full suspension system tied together with the chassis (rolling chassis). This prototype will be build will all tested results from prototype 1.

Plan for Tests on Prototype

Prototype 1 will involve numerous driving tests. These tests will have multiple purposes including testing for the 2014 competition, driver training & driving of specific circuits in order to test vehicle dynamics. For FSAE competition testing, prototype 1 will be tested in an acceleration, braking and skid pad event. In order to test vehicle dynamics a 350-ft. slalom with seven gates spaced 50 ft. apart, a 100-ft.-diameter skid pad and a 0-60-0 mph course will be set up. The slalom will test the vehicles roll stiffness, steering response, bump steer, self steer or self aligning torque, tire grip, spring rates and vehicle alignment setup. The 100 ft diameter skid pad will also be testing vehicles lateral grip and roll center. The acceleration and brake tests involve the vehicles anti squat geometry and spring rate set ups. Based on all these results prototype 2 will be designed.

For prototype 2, the vehicle will only be completed to the rolling chassis stage. The instructions and procedure will be left for the 2015 FIU SAE test to conduct testing when prototype 2 is fully functioning as a driving vehicle. The tilt test can also be conducted testing the vehicles rollover stability requirements.

Conclusion

As seen before, the chassis and suspension will be an improvement based off of 2012 and 2013 designs. The Chassis will be lighter and more rigid. Suspension will be constructed more rigid with improvement of vehicle dynamics for a performance autocross style race. Also, all safety factors will be calculated and proper hardware will be used throughout the whole design

(grade 8, SAE hardware). Finally the chassis and suspension will be an improvement for the 2015 formula SAE team and competition.

References

Beckman, B. (1991). *The Physics of Racing.* Burbank, CA.
Gillespie, T. D. (1992). *Fundamentals of Vehicle Dynamics.* Warrendale, PA: SAE International.
Goryca, J. E. (2010). *Force* and *Moment Plots from Pacejka 2002.* U.S. Army Tank-automotive and Armaments Research Development and.
Smith, C. (1978). *Tune to Win.* Aero Publishers.
Smith, C. (1984). *Engineer to Win.* Motorbooks.
William F. Milliken, D. L. (1995). *Race Car Vehicle Dynamics.* Warrendale, PA: SAE International.

Appendix A: 2015 FSAE Rules

Have not been released yet

Appendix B: Hoosier .TIR file

```
FILE_TYPE             ='tir'
FILE_VERSION           = 3.0
FILE_FORMAT            ='ASCII'
! : TIRE_VERSION :     PAC2002
! : COMMENT :          Stackpole Engineering Services, Inc.
! : COMMENT :          Created By : Melissa Patterson
! : COMMENT :          September 4, 2012
! : COMMENT :          Customer     : FSAE
! : COMMENT :          Construction : 6.0 / 18.0 - 10
! : COMMENT :          DOT : XXXXXX
! : COMMENT :          Position     : All
! : COMMENT :          Manufacturer : Hoosier
! : COMMENT :          Nom. section width(in)  8.10
! : COMMENT :          Nom. aspect ratio       0.667
! : COMMENT :          Infl. pressure   (Psi)  12.0
! : COMMENT :          Rim Diameter     (in)  10.0
! : COMMENT :          Rim Width        (in)   7.0
! : COMMENT :          Test speed      (mph)  45.0
! : FILE FORMAT :      ASCII
! USE_MODE specifies the type of calculation performed:
!      0: Fz only, no Magic Formula evaluation
!      1: Fx,My only
!      2: Fy,Mx,Mz only
!      3: Fx,Fy,Mx,My,Mz uncombined force/moment calculation
!      4: Fx,Fy,Mx,My,Mz combined force/moment calculation
!    +10: including relaxation behavior
!    *-1: mirroring of tyre characteristics
!
!      example: USE_MODE = -12 implies:
!      -calculation of Fy,Mx,Mz only
!      -including relaxation effects
!      -mirrored tyre characteristics
!
$----------------------------------------------------------------units
[UNITS]
 LENGTH            = 'meter'
 FORCE             = 'Newton'
 ANGLE             = 'radians'
 MASS              = 'kg'
 TIME              = 'second'
$----------------------------------------------------------------model
[MODEL]
```

```
PROPERTY_FILE_FORMAT    ='PAC2002'
USE_MODE              = 14              $Tyre use switch (IUSED)
VXLOW                 = 1
LONGVL                = 20.1168          $Measurement speed
TYRESIDE              = 'RIGHT'          $Mounted side of tyre at vehicle/test bench
$----------------------------------------------------------dimensions
[DIMENSION]
UNLOADED_RADIUS       = 0.2286           $Free tyre radius
WIDTH                 = 0.2057           $Nominal section width of the tyre
ASPECT_RATIO          = 0.6670           $Nominal aspect ratio
RIM_RADIUS            = 0.1270           $Nominal rim radius
RIM_WIDTH             = 0.1778           $Rim width
$-----------------------------------------------------------------shape
[SHAPE]
{radial width}
 1.0   0.0
 1.0   0.4
 1.0   0.9
 0.9   1.0
$----------------------------------------------------------parameter
[VERTICAL]
VERTICAL_STIFFNESS    =  96665.00        $Tyre vertical stiffness
VERTICAL_DAMPING      = 48332.5          $Tyre vertical damping
BREFF                 = 0.2286           $Low load stiffness e.r.r.
DREFF                 = 0.2186           $Peak value of e.r.r.
FREFF                 = 0.3000           $High load stiffness e.r.r.
FNOMIN                = 559.1386                    $Nominal wheel load
$-----------------------------------------------------long_slip_range
[LONG_SLIP_RANGE]
KPUMIN                = -0.5000          $Minimum valid wheel slip
KPUMAX                =  0.5000          $Maximum valid wheel slip
$-----------------------------------------------------slip_angle_range
[SLIP_ANGLE_RANGE]
ALPMIN                = -0.2094          $Minimum valid slip angle
ALPMAX                =  0.2094          $Maximum valid slip angle
$-------------------------------------------inclination_slip_range
[INCLINATION_ANGLE_RANGE]
CAMMIN                = 0.0000                      $Minimum valid camber angle
CAMMAX                =  0.0698                     $Maximum valid camber angle
$-------------------------------------------------vertical_force_range
[VERTICAL_FORCE_RANGE]
FZMIN                 =   222.4          $Minimum allowed wheel load
FZMAX                 =   1556.8         $Maximum allowed wheel load
$-----------------------------------------------------------scaling
[SCALING_COEFFICIENTS]
```

```
 LFZO             = 1.0            $Scale factor of nominal (rated) load
 LCX              = 1.0            $Scale factor of Fx shape factor
 LMUX             = 1.0            $Scale factor of Fx peak friction coefficient
 LEX              = 1.0            $Scale factor of Fx curvature factor
 LKX              = 1.0            $Scale factor of Fx slip stiffness
 LHX              = 1.0            $Scale factor of Fx horizontal shift
 LVX              = 1.0            $Scale factor of Fx vertical shift
 LGAX             = 1.0            $Scale factor of camber for Fx
 LCY              = 1.0            $Scale factor of Fy shape factor
 LMUY             = 1.0            $Scale factor of Fy peak friction coefficient
 LEY              = 1.0            $Scale factor of Fy curvature factor
 LKY              = 1.0            $Scale factor of Fy cornering stiffness
 LHY              = 1.0            $Scale factor of Fy horizontal shift
 LVY              = 1.0            $Scale factor of Fy vertical shift
 LGAY             = 1.0            $Scale factor of camber for Fy
 LTR              = 1.0            $Scale factor of peak of pneumatic trail
 LRES             = 1.0            $Scale factor for offset of residual torque
 LGAZ             = 1.0            $Scale factor of camber for Mz
 LXAL             = 1.0            $Scale factor of alpha influence on Fx
 LYKA             = 1.0            $Scale factor of alpha influence on Fx
 LVYKA            = 1.0            $Scale factor of kappa induced Fy
 LS               = 1.0            $Scale factor of moment arm of Fx
 LSGKP            = 1.0            $Scale factor of relaxation length of Fx
 LSGAL            = 1.0            $Scale factor of relaxation length of Fy
 LGYR             = 1.0            $Scale factor of gyroscopic torque
 LMX              = 1.0            $Scale factor of overturning couple
 LVMX             = 1.0            $Scale factor of Mx vertical shift
 LMY              = 1.0            $Scale factor of rolling resistance torque
$----------------------------------------------------------LONGITUDINAL_FORCE
[LONGITUDINAL_COEFFICIENTS]
 PCX1             =  1.27872550E+00   $Shape factor Cfx for longitudinal force
 PDX1             = -3.51415830E+00   $Longitudinal friction Mux at Fznom
 PDX2             =  6.33383390E-01   $Variation of friction Mux with load
 PDX3             =  7.11629130E+00   $Variation of friction Mux with camber
 PEX1             =  1.34635150E+00   $Longitudinal curvature Efx at Fznom
 PEX2             =  3.84490190E-17   $Variation of curvature Efx with load
 PEX3             = -3.92323870E-17   $Variation of curvature Efx with load squared
 PEX4             =  7.42710500E-03   $Factor in curvature Efx while driving
 PKX1             =  5.85243740E+01   $Longitudinal slip stiffness Kfx/Fz at Fznom
 PKX2             =  5.47564740E+00   $Variation of slip stiffness Kfx/Fz with load
 PKX3             = -4.10850790E-01   $Exponent in slip stiffness Kfx/Fz with load
 PHX1             =  2.14075670E-02   $Horizontal shift Shx at Fznom
 PHX2             =  2.27382190E-02   $Variation of shift Shx with load
 PVX1             = -1.65597580E-01   $Vertical shift Svx/Fz at Fznom
 PVX2             = -3.76003610E-02   $Variation of shift Svx/Fz with load
```

```
 RBX1            =  2.18035740E+01    $Slope factor for combined slip Fx reduction
 RBX2            = -6.29073440E+00    $Variation of slope Fx reduction with kappa
 RCX1            =  5.16330770E+00    $Shape factor for combined slip Fx reduction
 REX1            =  3.14293760E+00    $Curvature factor of combined Fx
 REX2            = -2.19035810E-01    $Curvature factor of combined Fx with load
 RHX1            = -1.76110940E-02    $Shift factor for combined slip Fx reduction
 PTX1            =  0.00000000E+00    $Relaxation length SigKap0/Fz at Fznom
 PTX2            =  0.00000000E+00    $Variation of SigKap0/Fz with load
 PTX3            =  0.00000000E+00    $Variation of SigKap0/Fz with exponent of load
$----------------------------------------------------OVERTURNING_MOMENT
[OVERTURNING_COEFFICIENTS]
 QSX1            = -5.37765690E-05    $Lateral force induced overturning moment
 QSX2            =  1.34243430E+00    $Camber induced overturning couple
 QSX3            =  4.55659640E-02    $Fy induced overturning couple
$-------------------------------------------------------------LATERAL_FORCE
[LATERAL_COEFFICIENTS]
 PCY1            =  1.61114770E+00    $Shape factor Cfy for lateral forces
 PDY1            = -2.56461540E+00    $Lateral friction Muy
 PDY2            =  1.98332500E-01    $Variation of friction Muy with load
 PDY3            =  7.88890470E+00    $Variation of friction Muy with squared camber
 PEY1            =  5.99405940E-01    $Lateral curvature Efy at Fznom
 PEY2            = -1.05328300E-02    $Variation of curvature Efy with load
 PEY3            = -5.09521880E-01    $Zero order camber dependency of curvature Efy
 PEY4            = -4.95122130E+00    $Variation of curvature Efy with camber
 PKY1            = -5.58259490E+01    $Maximum value of stiffness Kfy/Fznom
 PKY2            =  2.32682900E+00    $Load at which Kfy reaches maximum value
 PKY3            =  8.28589030E-01    $Variation of Kfy/Fznom with camber
 PHY1            =  4.37208140E-03    $Horizontal shift Shy at Fznom
 PHY2            =  1.84739710E-03    $Variation of shift Shy with load
 PHY3            =  7.65552290E-02    $Variation of shift Shy with camber
 PVY1            =  3.68120950E-02    $Vertical shift in Svy/Fz at Fznom
 PVY2            =  9.40894990E-03    $Variation of shift Svy/Fz with load
 PVY3            =  4.72409040E-02    $Variation of shift Svy/Fz with camber
 PVY4            = -2.07519840E+00    $Variation of shift Svy/Fz with camber and load
 RBY1            =  2.64974160E-02    $Slope factor for combined Fy reduction
 RBY2            = -2.60705200E+02    $Variation of slope Fy reduction with alpha
 RBY3            =  5.81120430E-02    $Shift term for alpha in slope Fy reduction
 RCY1            =  4.83367230E+02    $Shape factor for combined Fy reduction
 REY1            = -4.10563800E+01    $Curvature factor of combined Fy
 REY2            =  1.84129220E+00    $Curvature factor of combined Fy with load
 RHY1            =  3.52670620E-02    $Shift factor for combined Fy reduction
 RHY2            =  2.56134790E-02    $Shift factor for combined Fy reduction with load
 RVY1            =  1.62049310E-01    $Kappa induced side force Svyk/Muy*Fz at Fznom
 RVY2            = -1.43867580E+00    $Variation of Svyk/Muy*Fz with load
 RVY3            =  1.14411730E+02    $Variation of Svyk/Muy*Fz with camber
```

```
 RVY4             = -2.77924030E+02     $Variation of Svyk/Muy*Fz with alpha
 RVY5             = -3.34090680E+02     $Variation of Svyk/Muy*Fz with kappa
 RVY6             = -6.78885500E-04     $Variation of Svyk/Muy*Fz with atan (kappa)
 PTY1             =  0.00000000E+00     $Peak value of relaxation length SigAlp0/R0
 PTY2             =  0.00000000E+00     $Value of Fz/Fznom where SigAlp0 is extreme
$----------------------------------------------------ROLLING_COEFFICIENTS
[ROLLING_COEFFICIENTS]
 QSY1             = 0.00000000E+00      $Rolling resistance torque coefficient
 QSY2             = 0.00000000E+00      $Rolling resistance torque depending on Fx
 QSY3             = 0.00000000E+00      $Rolling resistance torque depending on speed
 QSY3             = 0.00000000E+00      $Rolling resistance torque depending on speed ^4
$----------------------------------------------------------ALIGNING_TORQUE
[ALIGNING_COEFFICIENTS]
 QBZ1             =  7.61480610E+00     $Trail slope factor for trail Bpt at Fznom
 QBZ2             = -1.90805210E-01     $Variation of slope Bpt with load
 QBZ3             = -1.27311830E+00     $Variation of slope Bpt with load squared
 QBZ4             = -1.33931020E+00     $Variation of slope Bpt with camber
 QBZ5             =  2.73790000E+00     $Variation of slope Bpt with absolute camber
 QBZ9             =  2.22413510E-02     $Slope factor Br of residual torque Mzr
 QBZ10            = -1.72808380E-03     $Slope factor Br of residual torque Mzr
 QCZ1             =  1.49377510E+00     $Shape factor Cpt for pneumatic trail
 QDZ1             =  1.02952700E-01     $Peak trail Dpt" = Dpt*(Fz/Fznom*R0)
 QDZ2             = -1.92507310E-02     $Variation of peak Dpt" with load
 QDZ3             =  1.60096060E-01     $Variation of peak Dpt" with camber
 QDZ4             =  4.13584470E-01     $Variation of peak Dpt" with camber squared
 QDZ6             = -5.18597130E-02     $Peak residual torque Dmr" = Dmr/(Fz*R0)
 QDZ7             = -1.64092170E-02     $Variation of peak factor Dmr" with load
 QDZ8             =  2.44331100E-02     $Variation of peak factor Dmr" with camber
 QDZ9             = -2.52544490E-02     $Variation of peak factor Dmr" with camber and
load
 QEZ1             =  1.18165390E-01     $Trail curvature Ept at Fznom
 QEZ2             =  5.58891310E-02     $Variation of curvature Ept with load
 QEZ3             = -2.02787090E-01     $Variation of curvature Ept with load squared
 QEZ4             = -9.88809180E-01     $Variation of curvature Ept with sign of Alpha-t
 QEZ5             = -2.44285500E+01     $Variation of Ept with camber and sign Alpha-t
 QHZ1             =  8.98785560E-03     $Trail horizontal shift Sht at Fznom
 QHZ2             =  2.98264710E-04     $Variation of shift Sht with load
 QHZ3             = -1.39465090E-02     $Variation of shift Sht with camber
 QHZ4             =  6.68692620E-03     $Variation of shift Sht with camber and load
 SSZ1             =  0.00000          $Nominal value of s/R0: effect of Fx on Mz
 SSZ2             =  0.00000          $Variation of distance s/R0 with Fy/Fznom
 SSZ3             =  0.00000          $Variation of distance s/R0 with camber
 SSZ4             =  0.00000          $Variation of distance s/R0 with load and camber
 QTZ1             =  0               $Gyration torque constant
 MBELT            =  0               $Belt mass of the wheel
```

Appendix C: Formulas for Pacejka Fitting Constants

From (Goryca, 2010)

Longitudinal Force Fx

$$F_x = (D_x \sin[C_x \arctan\{B_x\kappa_x - E_x(B_x\kappa_x - \arctan(B_x\kappa_x))\}] + SV_x)\cdot G_{x\alpha}$$

Where

$$\kappa_x = \kappa + SH_x$$
$$C_x = P_{Cx1}\lambda_{Cx}$$
$$D_x = \mu_x F_z$$
$$\mu_x = (P_{Dx1} + P_{Dx2}df_z)\left(1 - P_{Dx3}\gamma^2\right)\lambda_{\mu_y}$$
$$E_x = (P_{Ex1} + P_{Ex2}df_z + P_{Ex3}df_z^2)\left(1 - P_{Ex4}sgn(\kappa_x)\right)\lambda_{Ex}$$
$$K_{x\kappa} = (P_{Kx1} + P_{Kx2}df_z)\exp(P_{Kx3}df_z)F_z\lambda_{K\kappa}$$
$$B_x = \frac{K_{x\kappa}}{C_x D_x}$$
$$S_{Hx} = (P_{Hx1} + P_{Hx2}df_z)\lambda_{Hx}$$
$$S_{Vx} = F_z(P_{Vx1} + P_{Vx2}df_z)\lambda_{Vx}\lambda_{\mu_x}$$

Combined Slip:

$$G_{x\alpha} = \frac{\cos[C_{x\alpha}\arctan\{B_{x\alpha}\alpha_s - E_{x\alpha}(B_{x\alpha}\alpha_s - \arctan(B_{x\alpha}\alpha_s))\}]}{\cos[C_{x\alpha}\arctan\{B_{x\alpha}S_{Hx\alpha} - E_{x\alpha}(B_{x\alpha}S_{Hx\alpha} - \arctan(B_{x\alpha}S_{Hx\alpha}))\}]}$$

Where

$$\alpha_s = \alpha_F + S_{Hx\alpha}$$
$$B_{x\alpha} = (r_{Bx1} + r_{Bx3}\gamma^2)\cos\{\arctan[r_{Bx2}\kappa]\}\lambda_{x\alpha}$$
$$C_{x\alpha} = r_{Cx1}$$
$$E_{x\alpha} = r_{Ex1} + r_{Ex2}df_z$$
$$S_{Hx\alpha} = r_{Hx1}$$

For pure slip, Gxα = 1.

Lateral force Fy

$$F_y = G_{y\kappa}F_{yp} + S_{Vy\kappa}$$

Where

$$F_{yp} = (D_y \sin[C_y \arctan\{B_y\alpha_y - E_y(B_y\alpha_y - \arctan(B_y\alpha_y))\}] + S_{Vy})$$
$$\alpha_y = \alpha_F + S_{Hy}$$
$$C_y = P_{Cy1}\lambda_{Cy}$$
$$D_y = \mu_y F_z$$
$$\mu_y = (P_{Dy1} + P_{Dy2}df_z)(1 - P_{Dy3}\gamma^2)\lambda_{\mu_y}$$
$$E_y = (P_{Ey1} + P_{Ey2}df_z)\left(1 + P_{Ey5}\gamma^2 - (P_{Ey3} + P_{Ey4})sgn(\alpha_y)\right)\lambda_{Ey}$$
$$K_{y\alpha} = P_{Ky1}F_{z0}\sin\left[P_{Ky4}\arctan\left\{\frac{F_z}{(P_{Ky2} + P_{Ky5}\gamma^2)F_{z0}}\right\}\right](1 - P_{Ky3}|\gamma|)\lambda_{Ky\alpha}$$
$$B_y = \frac{K_{y\alpha}}{C_y D_y}$$
$$S_{Hy} = S_{Hy0} + S_{Hy\gamma}$$
$$S_{Hy0} = (P_{Hy1} + P_{Hy2}df_z)\lambda_{Hy}$$
$$S_{Hy\gamma} = \frac{K_{y\gamma} - S_{Vy\gamma}}{K_{y\alpha}}$$
$$S_{Vy0} = F_z(P_{Vy1} + P_{Vy2}df_z)\lambda_{Vy}\lambda_{\mu_y}$$
$$S_{Vy\gamma} = F_z(P_{Vy3} + P_{Vy4}df_z)\gamma\lambda_{Ky\gamma}\lambda_{\mu_y}$$
$$S_{Vy\kappa} = D_{Vy\kappa}\sin(r_{Vy5}\arctan(r_{Vy6}\kappa))\lambda_{Vy\kappa}$$
$$D_{Vy\kappa} = \mu_y F_z(r_{Vy1} + r_{Vy2}df_z + r_{Vy3}\gamma)\cos(\arctan(r_{Vy4}\alpha_F))$$

Combined Slip:

$$G_{y\kappa} = \frac{\cos\left[C_{y\kappa}\arctan\left\{B_{y\kappa}\kappa_s - E_{y\kappa}\left(B_{y\kappa}\kappa_s - \arctan(B_{y\kappa}\kappa_s)\right)\right\}\right]}{\cos\left[C_{y\kappa}\arctan\left\{B_{y\kappa}S_{Hy\kappa} - E_{y\kappa}\left(B_{y\kappa}S_{Hy\kappa} - \arctan(B_{y\kappa}S_{Hy\kappa})\right)\right\}\right]}$$

Where

$$\kappa_s = \kappa_F + S_{Hx\kappa}$$
$$B_{y\kappa} = (r_{By1} + r_{By4}\gamma^2)\cos\{\arctan[r_{Bx2}(\alpha - r_{By3})]\}\lambda_{y\kappa}$$
$$C_{y\kappa} = r_{Cy1}$$
$$E_{y\kappa} = r_{Ey1} + r_{Ey2}df_z$$
$$S_{Hy\kappa} = r_{Hy1} + r_{Hy2}df_z$$

For pure slip, SVyκ = 0, Gyκ = 1.

Overturning moment Mx

$$M_x = R_0 F_z \lambda_{Mx} \left(Q_{Sx1} \lambda_{Mx} - Q_{Sx2} \gamma + \frac{Q_{Sx3} F_y}{F_{z0}} \right)$$

Rolling resistance My

For tire data where FITTYP is equal to 5:

$$M_y = R_0 (S_{Vx} + K_x S_{Hx})$$

Otherwise:

$$M_y = -R_0 F_{z0} \lambda_{My} \left\{ \left(Q_{Sy1} + \frac{Q_{Sy2} F_x}{F_{z0}} + Q_{Sy3} \left| \frac{V_x}{V_{ref}} \right| \right) + Q_{Sy4} \left(\frac{V_x}{V_{ref}} \right)^4 \right\}$$

Self aligning moment Mz

$$M_z = -t \cdot F_{y0} + M_{zr}$$

Where

$$S_{Ht} = Q_{Hz1} + Q_{Hz2} df_z + (Q_{Hz3} + Q_{Hz4} df_z) \lambda_z$$
$$\alpha_t = \alpha + S_{Ht}$$
$$t = D_t \cos\left(C_t \arctan\left(B_t \alpha_t - E_t (B_t \alpha_t - \arctan(B_t \alpha_t))\right)\right) \cdot \cos(\alpha)$$
$$\alpha_r = \alpha + S_{Hf}$$
$$M_{zr} = D_r \cos\left(C_r \arctan(B_r \alpha_r)\right) \cdot \cos(\alpha)$$
$$\gamma_z = \gamma \lambda_{\gamma z}$$
$$B_t = (Q_{Bz1} + Q_{Bz2} df_z + Q_{Bz3} df_z^2)(1 + Q_{Bz4} \gamma_z + Q_{Bz5} |\gamma_z|) \lambda_{Ky} / \lambda_{\mu y}$$
$$C_t = Q_{Cz1}$$
$$D_t = F_z (Q_{Dz1} + Q_{Dz2} df_z)(1 + Q_{Dz3} \gamma_z + Q_{Dz4} \gamma_z^2)(R_0 / F_{z0}) \lambda_t$$
$$E_t = (Q_{Ez1} + Q_{Ez2} df_z + Q_{Ez3} df_z^2) \left(1 + (Q_{Ez4} + Q_{Ez5} \gamma_z) \cdot \frac{2}{\pi} \cdot \arctan(B_t C_t \alpha_t)\right) \text{ with } E_t \leq 1$$
$$B_r = Q_{Bz9} \frac{\lambda_{Ky}}{\lambda_{\mu y}} + Q_{Bz10} B_y C_y$$
$$C_r = 1$$
$$D_r = F_z \left((Q_{Dz6} + Q_{Dz7} df_z) \lambda_r + (Q_{Dz8} + Q_{Dz9} df_z) \lambda_z \right) R_0 \lambda_{\mu y}$$